Biodegradable Nanoparticles Containing Benzopsoralens: An Attractive Strategy for Modifying Vascular Function in Pathological Skin Disorders

Anderson J. Gomes,[1] Laurelúcia O. Lunardi,[2] Flavio H. Caetano,[2] Antonio Eduardo H. Machado,[3] Ana Maria F. Oliveira-Campos,[4] Lusiane M. Bendhack,[5] Claure N. Lunardi[1]

[1]*Universidade de Brasília, Faculdade de Ceilândia, QNN-14 AE CEI, 72220-140 Ceilândia, DF, Brazil*
[2]*Instituto de Biociência, Universidade Estadual Paulista Júlio de Mesquita Filho, 13506-900 Rio Claro, SP, Brazil*
[3]*Instituto de Química, Universidade Federal de Uberlândia, 38400-089 Uberlândia, MG, Brazil*
[4]*Centro de Química, Universidade do Minho, Campus Gualtar, P-4710-057 Braga, Portugal*
[5]*Faculdade de Ciências Farmacêuticas de Ribeirão Preto, Av do Café s/n, 14040-903 Ribeirão Preto, SP, Brazil*

Received 22 May 2010; accepted 22 September 2010
DOI 10.1002/app.33427
Published online 3 March 2011 in Wiley Online Library (wileyonlinelibrary.com).

ABSTRACT: Psoralens are often used to treat skin disorders such as psoriasis, vitiligo, and others. The toxicity and fast degradation of these drugs can be diminished by encapsulation in drug-delivery systems (DDS). Nanoparticles (NPs) containing the benzopsoralen (BP) (3-ethoxy carbonyl-2H-benzofuro[3,2-e]-1-benzopiran-2-one) were prepared by the solvent-evaporation technique, and parameters such as particle size, zeta potential, drug-encapsulation efficiency, and external morphology were evaluated. The analysis revealed that the NPs are spherical and with smooth external surface with diameter of 815 ± 80 nm, they present low tendency toward aggregation, and the encapsulation efficiency was of 74%. The intracellular distribution of NPs as well as their uptake by tissues was monitored by using laser confocal microscopy and transmission electron microscopy (TEM). The use of a BP in association with ultraviolet light (360 nm) revealed by TEM morphological characteristics of cell damage such as cytosolic vesiculation, mitochondria condensation, and swelling of both the granular endoplasmic reticulum and the nuclear membrane. The primary target of DDS and drugs in vascular system are endothelial cells and an attractive strategy for modifying vascular function in various pathological states of skin disorders, cancer, and inflammation. The results presented in this work indicate that poly(lactic-*co*-glycolic acid) NP should be a promising sustained release for BP for systemic and local delivery associated with ultraviolet irradiation (PUVA therapy).
 J Appl Polym Sci 121: 1348–1354, 2011

Key words: nanoparticles; biological applications of polymers; drug-delivery system; microencapsulation; TEM

INTRODUCTION

The association of psoralens with UVA irradiation (320–400 nm) is currently being used in dermatology (orally or topically). This combination is known as PUVA therapy.[1–10] This treatment is effective against diseases such as vitiligo, psoriasis, mycosis fungoides, and atopic eczema, among others.[11–19]

The skin consists of five layers (deepest to most superficial): the stratum basale, the stratum spinosum, the stratum granulosum, the stratum lucidum, and the stratum corneum. It is also composed of four different types of cells: keratinocytes, melanocytes, Langerhan's, and Merkel cells.[20] Typically, it takes about 4 weeks for cells to move from the stratum basale toward the stratum corneum.[20] The keratinocytes in the basal layer divide once every 13–14 days.[20,21] The surface cells slough off and are replaced by the underlying cells. In psoriatic skin, the cell cycle accelerates and the cells divide every 1.5 days, with maturation and shedding occurring in 4 days. Because the cells move to the surface so rapidly, they do not differentiate, thus forming scaly, inflamed, red skin.[20,21]

Most psoriasis drug development has focused on the T lymphocyte and its cytokines, which have been implicated in the changes seen in the skin of patients with psoriasis, including capillary dilation, epidermal ridge dilation, neutrophil proliferation, and plaque formation.[22–25]

The physicochemical properties of drugs such as molecular weight, shape, charge, and aqueous solubility determine the rate of diffusion through tissue.[26]

The photophysical properties of the benzopsoralen (BP) have been recently investigated,[9,27,28] and it has been shown that they can photochemically sensitize the generation of singlet oxygen with a quantum

Correspondence to: A. J. Gomes (ajgomes@unb.br) or C. N. Lunardi (clunardi@unb.br).
Contract grant sponsors: DPP-UnB, FAP-DF, CNPq, CAPES, FAPEMIG, FAPESP.

efficiency approaching unity,[9] contrary to other compounds (8-methoxypsoralen, 5-methoxypsoralen, and trimethylpsoralen) usually used in PUVA therapy intercalating in DNA bases.[29–33] Unfortunately, most photosensitizing chemicals are also phototoxic to the skin, and skin contact with these molecules in the presence of UV irradiation results in sunburn, erythematic, and eventual edema,[10,34] thus limiting the use of PUVA therapy for topical treatment of skin disorders.[34–36]

A drug-delivery system (DDS) that may be used to enhance the action of PUVA therapy in special nanoparticles (NPs) has been investigated for the delivery of different types of therapeutic agents including proteins, peptides, and DNA.[37,38] In addition to providing sustained release, NPs can protect the encapsulated agent from enzymatic degradation.[39–41]

It is well known that endothelium is an important target for drugs, because it is involved in a number of normal and pathophysiological conditions such as angiogenesis, atherosclerosis, tumor growth, myocardial infarction, limb and cardiac ischemia, and restenosis.[42–45] In skin disorders such as psoriasis, there is now considerable evidence indicating that angiogenesis may, at least in part, play a role in increasing the psoriatic plaque.[46] Also, the demonstration of angiogenic activity in plaque skin has led some authors to investigate the possible benefits of antiangiogenic agents in the treatment of clinical lesions.[47,48] However, the delivery of agents that induce the destruction of the endothelial cells (ECs) in skin vasculature, activated by light irradiation, needs to be investigated. Thus, the main objective of this work is to evaluate the morphological changes of vasculature in the normal rat skin after BP–NP in local delivery associated with light irradiation. In this work, we analyzed the normal rat skin and used rat aorta as the mimetic vessel model to understand the uptake of the BP–NP by EC.

MATERIALS AND METHODS

Chemicals

Poly(D,L-lactic-*co*-glycolic acid) (PLGA) 50 : 50, M_w 17 kDa (Sigma), polyvinyl alcohol (PVA) (13–23 kDa, 87–89% hydrolyzed) (Aldrich), and analytical grade dichloromethane (Merck) were used as supplied. The fluorescent bezopsoralen 3-ethoxy carbonyl-2H-benzofuro[3,2-e]-1-benzopiran-2-one (BP) was synthesized and supplied by Oliveira-Campos, from Universidade do Minho. All other chemicals were of analytical grade and were used without further purification.

Preparation of NPs by the solvent evaporation technique

The nanoparticles (NPs) loaded or not with BP were prepared by solvent-evaporation method.[49,50] Typically, the organic phase consisted of 0.1 g of the PLGA 50 : 50 polymer and 10 m*M* of fluorescent BP dissolved in 10 mL of CH_2Cl_2. The dispersed phase was rather into the homogeneous aqueous phase [50 mL of an aqueous phase containing 1% (w/v) of 88% hydrolyzed PVA as dispersing agent] under ice cooling, using a high-speed homogenizer (Ultra-Turrax T18-S18*N*-19G, IKA) for 60 s at 14,000 rpm. Furthermore, solvent evaporation was carried out by gentle magnetic stirring at room temperature for a period of 3–5 h. NP was recovered by centrifugation for 5 min at 10,000 rpm and 4°C. They were then washed (three times) with distilled water and lyophilized (Labconco®, USA). NP without BP was prepared by the same procedure. Dried NP was stored in a sealed glass vial and placed in a dessicator kept at 4°C.

Particle size and surface charge (zeta potential)

Particle size and size distribution were determined by photon correlation spectroscopy using the quasi-elastic light scattering technique, in a Zetasizer 3000 equipment (Malvern Instrument) equipped with a 10 mW He–Ne 633 nm laser beam at 25°C and at a scattering angle of 90°. For the particle size analysis, a dilute suspension (1.0 mg mL^{-1}) of NP was prepared in double-distilled water and sonicated in an ice bath for 30 s. The zeta potential of the NPs in PBS buffer (0.1 m*M*, pH 7.4, and 1.0 mg/mL) was determined by using ZetaPlus™ in the zeta potential analysis mode.

Encapsulation efficiency

A weighed quantity of NPs was dissolved in methylene chloride. The BP content was assayed by spectrometry at 345 nm by using a calibration curve. The calibration curve for the quantification of BP was linear over the range of standard concentration between 1×10^{-7} and 1×10^{-3} mol L^{-1} with a correlation coefficient of $R^2 = 1.0$. The encapsulation efficiency was calculated as follows [eq. (1)]:

$$\text{Encapsulation efficiency}(\%) = \frac{\text{Amount of drug in microparticle}}{\text{Initial amount of drug}} \times 100 \quad (1)$$

NPs morphology: SEM analysis

Scanning electron microscopy (SEM) was used to evaluate the shape of PLGA nanoparticles (NPs). Samples were washed with sterile distilled water, fixed in 2.5% (v:v) glutaraldehyde (GA) in water, for 2 h, washed again with water, and dehydrated in a graded ethanol series and critical point dried. Samples containing NPs were mounted on aluminum

stubs and due to their lack of electrical conductivity, coated with 50-nm gold coating under an argon atmosphere. NPs were examined and photographed using an EVO 50 (Zeiss) scanning electron microscope operating at 20 kV in the traditional mode (SE1 detector).

Skin

Male Wistar rats weighing ~ 150 g ($n = 4$) were anesthetized with a mixture of halothane, N_2O, and O_2. After shaving and disinfection, 200 μL of a 25% suspension of BP–NP in 10 m*M* PBS, pH 7.4, was injected subcutaneously. At day 2, the rats were sacrificed, and the NPs with surrounding tissue, skin, and underlying muscle were carefully dissected. The samples were fixed in either of the fixative agents already described, during the time shown in brackets: formalin 4% (24 h); or mixture of formalin (4%) plus glutaraldehyde (0.1%) in PBS (12 h); or glutaraldehyde (2.5%) in PBS (6 h). After fixation, the samples were processed for microscopy analysis.

Transmission electron microscopy

For the transmission electron microscopy (TEM) studies, the samples were fixed in 2.5% glutaraldehyde in 0.1 mol L^{-1} sodium cacodylate buffer (pH 7.4) for 2 h at 25°C. The fixed cells were then post fixed in 1% osmium tetroxide in the same buffer for 1 h, dehydrated in a graded acetone series, and embedded in epoxy resin. Ultrathin sections were contrasted with alcoholic 2% uranyl acetate and 5% lead citrate. Ultrastructural examination was performed with a transmission electron microscope Philips CM-100 (Philips Electron Optics, Eindhoven, The Netherlands).

Visualization of cellular uptake by confocal laser scanning microscopy

Male Wistar rats (400–450 g) were killed by decapitation, and all the procedures are in accordance with the Ethical Animal Committee of the University of São Paulo, Brazil. The thoracic aorta was quickly removed, cleaned of adherent connective tissues, and cut into rings (100 ± 20 μm thick). To image arterial cross sections, the aorta rings were placed vertically in a coverslip covered with poly-L-lysine. The tissue was loaded with fluorescent BP–NP by incubation in the normal Hanks solution 120 min in CO_2 incubator. After washing with Hanks solution, the segment was placed on a chamber (1.0 mL in volume). The chamber was placed on the stage of a confocal microscope from the bottom of the chamber through a water-immersion objective (63×). Excitation wavelengths and emission were set according to the fluorescence properties of the drug (Ex. 488 nm/Em. 532 nm).

Irradiation

BP-loaded NPs (20 mg) were reconstituted with 2.0 mL of PBS pH 7.4 with 0.1% w/v Tween 80 in a glass vial, which was shaken and briefly bath-sonicated. About 1.5 mL of this suspension was then subcutaneously administered into the dorsolateral region of the neck. After 2 h, the region was irradiated using a 400-W mercury arc lamp was used as the irradiation source. A pass-band filter (Ocean Optics U360) filtered the radiation, ensuring that the samples were irradiated with light of 360 ± 10 nm (maximum transmittance 69%). Typical irradiances between 0.030 and 0.035 W/cm^2 were used to deliver a fluency of 1.0 J/cm^2. The irradiances were quantified using a PMA 2100 solar light radiometer. After light treatment, the cells were kept in the dark for 2 h. Nonirradiated cells were kept in the dark for the same period of time. The ambient light was <0.001 mW/cm^2. Both irradiated and nonirradiated cells were processed by TEM.

Statistical analysis

Statistical analysis of the results was carried out using Student's *t*-test.

RESULTS

NPs morphology: SEM analysis

The morphological analyses of the NPs were performed using scanning electron microscopy (SEM). Figure 1(A) shows a representative micrograph of a BP-loaded NPs, magnified at 20,000×. In all preparations reported in this work, the particles are spherical in shape, displaying a smooth surface. No meaningful difference was found between BP-loaded PLGA NPs and the empty NPs used as control. Figure 1(B) shows a laser scanning confocal microscopy of BP-loaded PLGA NPs excited with 488 nm.

Particle size and surface charge (zeta potential)

The distribution analyses (DLS) show a uniform size with varying diameters from 720 to 930 nm as presented in Figure 2 and confirmed by Figure 1.

The NPs colloidal stability was analyzed by measuring the NP zeta potential. In theory, more pronounced zeta potential values, either positive or negative, tend to stabilize particle suspension, because the electrostatic repulsion between particles with the

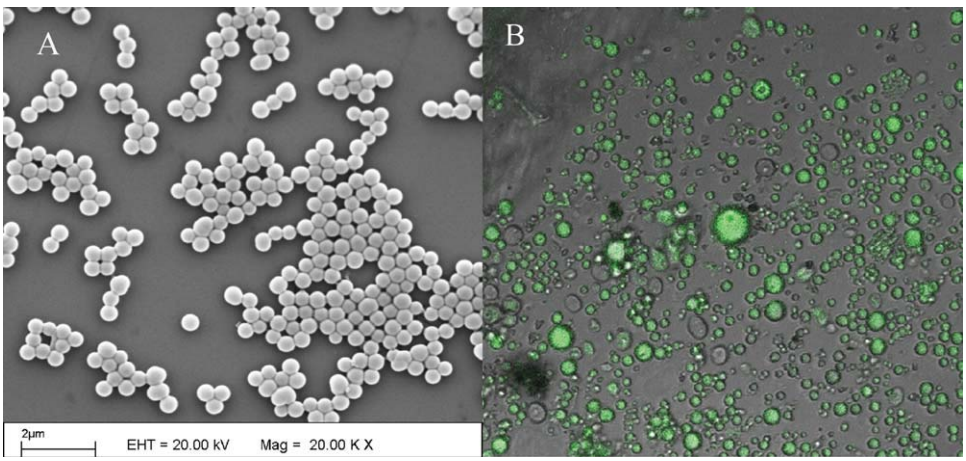

Figure 1 Scanning electron microscopy (SEM) of external morphology of nanoparticles loaded benzopsoralen, magnification of 20,000×. Scale bar corresponds to 2 μ*M*. (B) Laser Confocal Microscopy of BP-NP excited at 488 nm. [Color figure can be viewed in the online issue, which is available at wileyonlinelibrary.com.]

same electric charge prevents aggregation of the NPs. The particles consisting of PLGA-free dye were negatively charged (−3.2 mV at pH 7.4), whereas the zeta potential measured for the NPs loaded with BP was + 17.3 ± 2.9 mV.

Encapsulation efficiency

The drug-entrapment efficiency parameter was calculated from the experimentally determined actual drug loading of the NP and the theoretical drug loading. The values obtained by this method 74 ± 4% of incorporation.

TEM analysis

The histological evaluation of the vascular ECs loaded with NP–PB with/without UVA irradiation was done by TEM. In Figure 3(A), the transversal cut of the control rat skin without the NP and irradiated with light at 360 ± 10 nm, showing the intact vessel (black arrow-EC and bold arrow-myofibrils), is presented. In Figure 3(B), it is displayed that the endothelial and muscle cells loaded with BP–NP without light irradiation. This image shows no alteration in the cytoplasm of the EC. In Figure 3(C), the damage in the cytoplasm of EC promoted by the activation of NP–PB by irradiation (black arrow) is shown.

Laser confocal microscopy and image analysis

The uptake of BP–NP by ECs was evaluated in aorta rings as a model incubated for 120 min and imaged with a confocal microscope. As shown in Figure 4(A), phase contrast image of the aorta ring segment has undulation of the internal elastic membrane, which exists between vascular smooth muscle cells (square) and ECs-circle layers. The endothelial layer with the uptake BP–NP (arrows) was imaged in *xyz* mode 1024 × 1024 pixel at 700 Hz by a confocal scanning laser microscope (Leica TCS SP5). The BP–NP fluorescence was excited with the 488 nm line of an argon ion laser, and the emitted fluorescence was measured at 490–550 nm as shown in Figure 4(B). Serial *z*-sections of the cells, each 1 μm in thickness, demonstrated fluorescence activity in all the sections between 10 and 25 μm from the surface of the cells, indicating that the NPs were internalized by the cells and not simply bound to their surface (figure not shown). NPs were mostly seen localized in the EC as showed in merged image [Fig. 4(C)].

A major advantage of using the rat aorta artery segment was that SMCs and ECs were observed simultaneously at one confocal plane.

DISCUSSION

The BP was encapsulated in polymeric NPs of PLGA using the solvent-evaporation technique. The

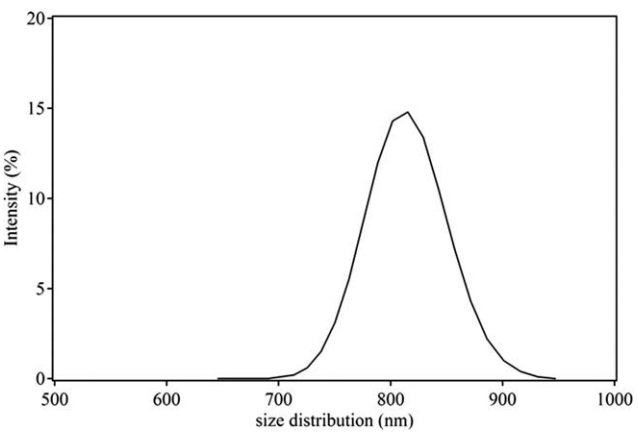

Figure 2 Size distribution profile (nm) of nanoparticles containing benzopsoralen.

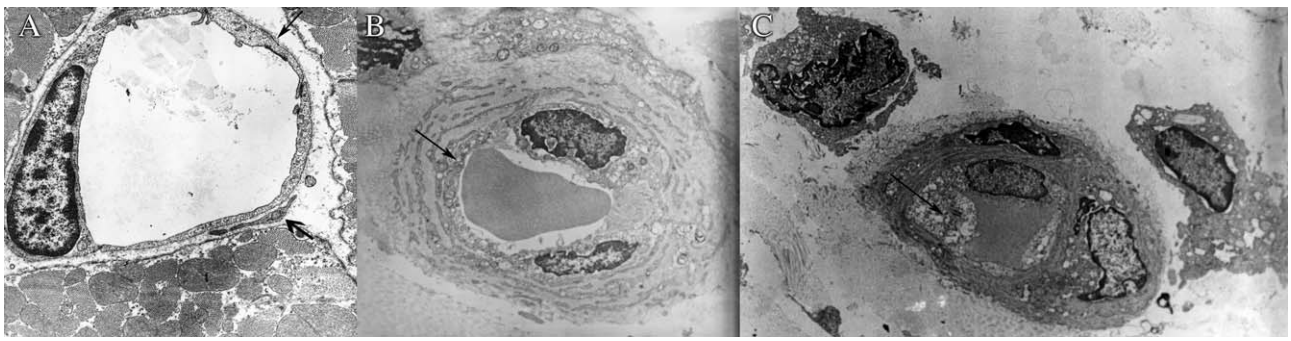

Figure 3 Transmission electron micrographs of (A) transversal cut of the control normal rat skin without BP-NP irradiated with 360 nm. (B) transversal cut of the rat skin loaded with BP-NP without irradiation and (C) transversal cut of the rat skin loaded with BP-NP after light irradiation.

choice of loading conditions was dictated by the characteristics of both BP and the NPs matrices. The BP is a hydrophobic compound with low-molecular weight, which makes it able to be used with the PLGA polymer. This polymer is biocompatible and biodegradable and also has been approved by the FDA for certain human clinical uses.[51–56]

The morphological analysis of the NPs was performed using SEM. In all preparations reported in this work, the particles are spherical in shape, displaying a smooth surface. No meaningful differences were found between the PLGA NPs containing BP (BP–NP) and the empty PLGA NPs used as control in relation to external morphology. Similar behavior has been described in relation to external morphology using different drugs loaded into nano and microparticles when the solvent-evaporation technique was applied.[50,57,58]

The success of this process depends primarily on the retention of the hydrophobic active compound within the polymer-containing organic phase from which the matrix is formed after evaporation of the solvent.[58–60] The high value (74%) of the BP entrapment efficiency for the NP is consistent with the hydrophobic character of the compound.

According to the literature,[61] the intravenous administration of particles with a diameter of several micrometers (larger than 6.0 μm) seems to be inefficient as a DDS because of its accumulation in lung capillaries and its difficult removal from the endothelial reticulum system.[51,61] The particle size significantly affects the level of cellular and tissue uptake, and in some cell lines, only submicron size particles are efficiently taken up.[35,62] In this respect, the size of particles is important and should be characterized carefully for skin subcutaneous administration. Solid lipid NP associated with psoralen showed an enhanced permeation in skin topically.[63] PLGA is a biodegradable and biocompatible polymer, currently being used by biomedical industry to produce biodegradable devices.[64] One of advantage of the use of these polymers is the modulation of size and porosity to drug delivery[65,66] as well as the possibility of systemically delivery.[67,68] The particles loaded with BP, evaluated by DLS, showed minimum dispersion size in submicron range. Therefore, this method

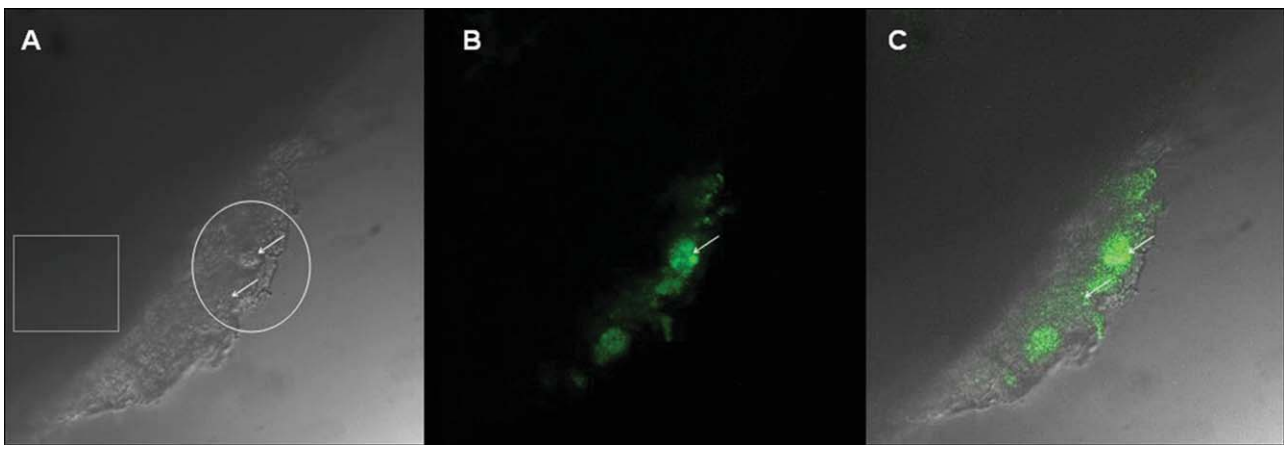

Figure 4 Cross section of a rat aorta artery segment by confocal microscope (A) image in differential contrast phase-DIC, (B) BP-NP fluorescence and (C) merge image. [Color figure can be viewed in the online issue, which is available at wileyonlinelibrary.com.]

resulted in the preparation of particles, suitable for the use as a DDS.

Using confocal microscopy, the BP–NP were visualized by its fluorescence emission displaying the drug entrapped in the NP. Once the ECs play an important role in the skin psoriasis inflammation process, in relation to capillary dilatation,[69] we used as a mimetic model a slice of aorta ring with endothelial layer to assess the BP–NP uptake by confocal microscopy. This uptake was also confirmed by TEM image of a subcutaneous skin loaded with BP–NP in the EC of a vessel, and the damage of this cell by BP–NP after light irradiation is promoted by photochemical process of BP generating singlet oxygen species.[9] Recently, it has been described for psoriasis treatment the use of antiangiogenic drugs suppressing EC migration in the inflammatory process.[70] This concept can be used and extrapolated to BP–NP usage as a complement for psoriasis treatment, acting in the microvasculature of the skin by decreasing the dilatation and epidermal ridge by photodamage.

CONCLUSIONS

In this study, the hydrophobic compound (3-ethoxy carbonyl-2H-benzofuro[3,2-e]-1-benzopiran-2-one) was encapsulated in a biodegradable polymer matrix (PLGA) to generate stable NPs. The present study demonstrates that the solvent evaporation method is a simple and suitable technique for the encapsulation of the hydrophobic compound, showing high-encapsulation efficiency. The results displayed a good batch to batch reproducibility with respect to the particle characteristics (size and size distribution, encapsulation efficiency, and release profile). In summary, the results of this study suggest that the NP prepared with PLGA may provide a sustained DDS useful for further application in psoriasis treatment.

References

1. Ito, T.; Aoshima, M.; Ito, N.; Uchiyama, I.; Sakamoto, K.; Kawamura, T.; Yagi, H.; Hashizume, H.; Takigawa, M. Arch Dermatol Res 2009, 301, 373.
2. Stern, R. S. N Engl J Med 2007, 357, 682.
3. Weber, F.; Schmuth, M.; Sepp, N.; Fritsch, P. Acta Derm-Venereol 2005, 85, 329.
4. Makki, S.; Muret, P.; Said, A. M.; Bassignot, P.; Humbert, P.; Agache, P.; Millet, J. Int J Pharm 1996, 133, 245.
5. Pires, A. L.; Honda, N. K.; Cardoso, C. A. L. J Pharm Biomed Anal 2004, 36, 415.
6. Gomes, A. J.; Faustino, A. S.; Lunardi, C. N.; Lunardi, L. O.; Machado, A. E. H. Int J Pharm 2007, 332, 153.
7. Canton, M.; Caffieri, S.; Dall' Acqua, F.; Di Lisa, F. FEBS Lett 2002, 522, 168.
8. Lysenko, E. P.; Melnikova, V. O.; Andina, E. S.; Wunderlich, S.; Pliquett, F.; Potapenko, A. Y. J Photochem Photobiol B 2000, 56, 187.
9. Machado, A. E. H.; Miranda, J. A.; Oliveira-Campos, A. M. F.; Severino, D.; Nicodem, D. E. J Photochem Photobiol A 2001, 146, 75.
10. Roop, S.; Guy, J.; Berl, V.; Bischoff, P.; Lepoittevin, J.-P. Bioorgan Med Chem 2004, 12, 3619.
11. Adisen, E.; Karaca, F.; Oztas, M.; Gurer, M. A. Clin Exp Dermatol 2008, 33, 344.
12. Serrano-Perez, J J; Gonzalez-Luque, R.; Merchan, M.; Serrano-Andres, L. J Photochem Photobiol A 2008, 199, 34.
13. Wackernagel, A.; Hofer, A.; Legat, F.; Kerl, H.; Wolf, P. Brit J Dermatol 2006, 154, 519.
14. Creamer, D.; Martyn-Simmons, C. L.; Osborne, G.; Kenyon, M.; Salisbury, J. R.; Devereux, S.; Pagliuca, A.; Ho, A. Y.; Mufti, G. J.; du Vivier, A. W. P. Arch Dermatol 2007, 143, 1157.
15. Gambichler, T. Arch Dermatol Res 2009, 301, 197.
16. Mariano, T. M.; Vetrano, A. M.; Gentile, S. L.; Heck, D. E.; Whittemore, M. S.; Guillon, C. D.; Jabin, I.; Rapp, R. D.; Heindel, N. D.; Laskin, J. D. Biochem Pharmacol 2002, 63, 31.
17. Saiad, A.; Makki, S.; Muret, P.; Humbert, P.; Millet, J. J. Dermatol Sci 1997, 14, 136.
18. Tatchen, J.; Kleinschmidt, M.; Marian, C. M. J Photochem Photobiol A: Chem 2004, 167, 201.
19. Tokura, Y. J Dermatol Sci 1999, 19, 114.
20. Peters, B. P.; Weissman, F. G.; Gill, M. A. Am J Health Syst Pharm 2000, 57, 645.
21. Greaves, M. W.; Weinstein, G. D. N Engl J Med 1995, 332, 581.
22. Baier, G.; Asadullah, K.; Zugel, U. Immunol Lett 2006, 105, 3.
23. Demidem, A.; Taylor, J. R.; Grammer, S. F.; Streilein, J. W. J Invest Dermatol 1991, 97, 454.
24. Dupuy, P.; Bagot, M.; Michel, L.; Descourt, B.; Dubertret, L. J. Invest Dermatol 1991, 96, 408.
25. Giblin, P. A.; Lemieux, R. M. Curr Pharm Design 2006, 12, 2771.
26. Minchinton, A. I.; Tannock, I. F. Nat Rev Cancer 2006, 6, 583.
27. Gomes, A. J.; Lunardi, C. N.; Lunardi, L. O.; Pitol, D. L.; Machado, A. E. H. Coordin Chem Rev 2011, 254, 355.
28. Oliveira, A. M. A. G.; Raposo, M. M. M.; Oliveira-Campos, A. M. F.; Machado, A. E. H. Helv Chim Acta 2003, 86, 2900.
29. Carter, D. M.; McMacken, M. L. V.; Condit, E. S. J. Invest Dermatol 1973, 60, 270.
30. Chen, W.; Lu, R. J. Microencapsulation 1999, 16, 551.
31. Collins, P.; Wainwrigth, N. J.; Amorin, N.; Lakshmipathi, T.; Fergusson, J. Brit J Dermatol 1996, 135, 248.
32. Legat, F. J.; Wolf, P.; Kränke, B. Brit J Dermatol 2001, 145, 821.
33. Man, I.; Dawe, R. S.; Ferguson, J.; Ibbotson, S.-H. Brit J Dermatol 2004, 151, 179.
34. Middelkamp-Hup, M. A.; Pathak, M. A.; Parrado, C.; Garcia-Caballero, T.; Rius-Díaz, F.; Fitzpatrick, T. B.; González, S. J Am Acad Dermatol 2004, 50, 41.
35. Gomes, A. J.; Faustino, A. S.; Machado, A. E. H.; Zaniquelli, M. E. D.; Rigoletto, T. D.; Lunardi, C. N.; Lunardi, L. O. Drug Deliv 2006, 13, 447.
36. Lindelöf, B.; Sigurgeirsson, B.; Tegner, E.; Larkö, O.; Johannesson, A.; Berne, B.; Ljunggren, B.; Andersson, T.; Mollin, L.; Nylander-Lundqvist, E.; Emtestam, L. Brit J Dermatol 1999, 141, 108.
37. Labhasetwar, V.; Song, C. X.; Levy, R. J. Adv Drug Deliv Rev 1997, 24, 63.
38. Labhasetwar, V.; Bonadio, J.; Goldstein, S. A.; Levy, J. R. Colloid Surf B 1999, 16, 281.
39. Alexis, F. Polym Int 2005, 54, 36.
40. Yoshioka, T.; Kawazoe, N.; Tateishi, T.; Chen, G. Biomaterials 2008, 29, 3438.
41. Hedley, M. L.; Curley, J.; Urban, R. Nat Med 1998, 4, 365.
42. Davda, J.; Labhasetwar, V. Int J Pharm 2002, 233, 51.
43. Dass, C. R.; Su, T. J. Pharm Pharmacol 2000, 52, 1301.
44. Martin, S. G.; Murray, J. C. Adv Drug Deliv Rev 2000, 41, 223.

45. Parikh, S. A.; Edelman, E. R. Adv Drug Deliv Rev 2000, 42, 139.
46. Hern, S.; Stanton, A. W. B.; Mellor, R. H.; Harland, C. C.; Levick, J. R.; Mortimer, P. S. Br J Dermatol 2005, 152, 505.
47. Atherton, D. J.; Wells, R. S.; Laurent, M. R.; Williams, Y. F. Brit J Dermatol 1980, 102, 307.
48. Dupont, E.; Falardeau, P.; Mousa, S. A.; Dimitriadou, V.; Pepin, M. C.; Wang, T. Q.; Alaoui-Jamali, M. A. Clin Exp Metastas 2002, 19, 145.
49. Gomes, A. J.; Lunardi, L. O.; Marchetti, J. M.; Lunardi, C. N.; Tedesco, A. C. Drug Deliv 2005, 12, 159.
50. Gomes, A. J.; Assuncao, R. M. N.; Rodrigues, G.; Espreafico, E. M.; Machado, A. E. D. J Appl Polym Sci 2007, 105, 964.
51. Gomes, A. D.; Lunardi, C. N.; Caetano, F. H.; Lunardi, L. O.; Machado, A. E. D. Microsc Microanal 2006, 12, 399.
52. Gomes, A. J.; Lunardi, L. O.; Marchetti, J. M.; Lunardi, C. N.; Tedesco, A. C. Photomed Laser Surg 2006, 24, 514.
53. Jain, R. A. Biomaterials 2000, 21, 2475.
54. Khang, G.; Rhee, J. M.; Jeong, J. K.; Lee, J. S.; Kim, M. S.; Cho, S. H.; Lee, H. B. Macromol Res 2003, 11, 207.
55. Sinha, V. R.; Trehan, A. Crit Rev Ther Drug 2005, 22, 535.
56. Thomas, V.; Dean, D. R.; Vohra, Y. K. Curr Nanosci 2006, 2, 155.
57. Mahdavi, H.; Mirzadeh, H.; Hamishehkar, H.; Jamshidi, A.; Fakhari, A.; Emami, J.; Najafabadi, A. R.; Gilani, K.; Minaiyan, M.; Najafi, M.; Tajarod, M.; Nokhodchi, A. J Appl Polym Sci 2011, 116, 528.
58. Mukerjee, A.; Vishwanatha, J. K. Anticancer Res 2009, 29, 3867.
59. Gomes, A. J.; Lunardi, C. N.; Tedesco, A. C. Photomed Laser Surg 2007, 25, 428.
60. Gomes, A. J.; Barbougli, P. A.; Espreafico, E. M.; Tfouni, E. J. Inorg Biochem 2008, 102, 757.
61. Jeon, H. J.; Jeong, J. I.; Jang, M. K.; Park, Y. H.; Nah, J. W. Int J Pharm 2000, 207, 99.
62. Panyam, J.; Labhasetwar, V. Adv Drug Deliv Rev 2003, 55, 329.
63. Fang, J. Y.; Fang, C. L.; Liu, C. H.; Su, Y. H. Eur J Pharm Biopharm 2008, 70, 633.
64. Kang, B. C.; Kang, K. S.; Lee, Y. S. Exp Anim Tokyo 2005, 54, 37.
65. Meneghello, G.; Parker, D. J.; Ainsworth, B. J.; Perera, S. P.; Chaudhuri, J. B.; Ellis, M. J.; De Bank, P. A. J Membr Sci 2009, 344, 55.
66. Wang, Y. J.; Shi, X. T.; Ren, L.; Wang, C. M.; Wang, D. A. Mater Sci Eng C-Bio S 2009, 29, 2502.
67. Jeong, Y. I.; Na, H. S.; Nah, J. W.; Lee, H. C. J Pharm Sci 2009, 98, 3659.
68. Rawat, A.; Majumder, Q. H.; Ahsan, F. J Control Release 2008, 128, 224.
69. Rosina, P.; Giovannini, A.; Gisondi, P.; Girolomoni, G. Skin Res Technol 2009, 15, 135.
70. Heidenreich, R.; Rocken, M.; Ghoreschi, K. Int J Exp Pathol 2009, 90, 232.